Regular Article

blood

LYMPHOID NEOPLASIA

SOX11 promotes tumor protective microenvironment interactions through CXCR4 and FAK regulation in mantle cell lymphoma

Patricia Balsas,[1,2,*] Jara Palomero,[1,*] Álvaro Eguileor,[1,2] Marta Leonor Rodríguez,[1] Maria Carmela Vegliante,[1] Ester Planas-Rigol,[1,3] Marta Sureda-Gómez,[1] Maria C. Cid,[1,3] Elias Campo,[1,2,4] and Virginia Amador[1,2]

[1]Institut d'Investigacions Biomèdiques August Pi i Sunyer (IDIBAPS), Barcelona, Spain; [2]Centro de Investigación Biomédica en Red de Cáncer (CIBERONC); and [3]Vasculitis Research Unit, Department of Autoimmune Diseases and [4]Department of Anatomic Pathology, Hospital Clínic, University of Barcelona, Barcelona, Spain

Key Points

- SOX11 regulates MCL homing and invasion via direct regulation of CXCR4 and FAK expression and PI3K/AKT and ERK1/2 signaling activation.
- SOX11 expression increases CAM-DR, contributing to a more aggressive MCL phenotype.

SOX11 overexpression in mantle cell lymphoma (MCL) has been associated with more aggressive behavior and worse outcome. However, SOX11 oncogenic pathways driving MCL tumor progression are poorly understood. Here, we demonstrate that SOX11 binds to regulatory regions of 2 important genes for microenvironment signals in cancer: (C-X-C motif) chemokine receptor 4 (*CXCR4*) and *PTK2* (encoding for focal adhesion kinase [FAK]). Moreover, SOX11$^+$ xenograft and human primary MCL tumors overexpress cell migration and stromal stimulation gene signatures compared with their SOX11$^-$ counterparts. We show that SOX11 directly upregulates CXCR4 and FAK expression, activating PI3K/AKT and ERK1/2 FAK-downstream pathways in MCL. Concordantly, SOX11$^+$ MCL cells have higher cell migration, transmigration through endothelial cells, adhesion to stromal cells, and cell proliferation and display an increased resistance to conventional drug therapies compared with SOX11$^-$ MCL cells. Specific FAK inhibition blocks downstream PI3K/AKT- and ERK1/2-mediated phosphorylation. Additionally, specific FAK and PI3K inhibitors reduce SOX11-enhanced MCL cell migration and stromal interactions and revert cell adhesion–mediated drug resistance (CAM-DR) to the same levels as SOX11$^-$ MCL cells. In intravenous MCL xenograft models, SOX11$^+$ MCL cells display higher cell migration, invasion, and growth compared with SOX11-knockdown cells, and specific FAK and CXCR4 inhibitors impair SOX11-enhanced MCL engraftment in bone marrow. Overall, our results suggest that SOX11 promotes MCL homing and invasion and increases CAM-DR through the direct regulation of CXCR4 and FAK expression and FAK/PI3K/AKT pathway activation, contributing to a more aggressive phenotype. Inhibition of this pathway may represent an efficient strategy to overcome stromal-mediated chemotherapy refractoriness in aggressive MCL. (*Blood*. 2017;130(4):501-513)

Introduction

Mantle cell lymphoma (MCL) is an aggressive lymphoid neoplasm characterized by extensive dissemination of tumor cells to lymphoid tissues, bone marrow (BM), peripheral blood (PB), and extranodal sites. Patients have short responses to current therapies and frequent relapses.[1,2] However, recent studies have identified a subset of MCL with indolent clinical behavior that tends to present with leukemic disease instead of extensive nodal infiltration, and patients may not need chemotherapy for long periods of time.[3-7] These cases have been recognized as "leukemic nonnodal MCL."[2] Molecular studies have identified *SOX11* (SRY [sex determining region-Y]-box11) as one of the best characterized discriminatory genes between these 2 clinicopathological subtypes of MCL.[8-10]

We recently proved that SOX11 silencing reduces tumor growth in a MCL xenograft model, consistent with the indolent clinical course of human SOX11$^-$ MCL.[11] SOX11 acts as an oncogene in MCL by promoting tumor angiogenesis through the PDGFA axis.[12] Moreover, we observed that the numbers of proangiogenic and prosurvival factors upregulated in SOX11$^+$ tumor xenografts were much larger than in their respective cell lines.[12] These results highlight the relevance of the crosstalk between MCL and accessory cells in the tumor microenvironment in the regulation of MCL aggressiveness and suggest that SOX11 may play a role in modulating tumor microenvironment prosurvival signals in MCL.

Although the mechanisms and signaling pathways of this tumorigenic event in MCL are poorly understood,[13-15] promising therapeutic approaches that disrupt crosstalk between the microenvironment and tumor cells to prevent the development of drug resistance and chemotherapy refractoriness are currently in early clinical development in patients with MCL.[16-21] In this study, we searched for potential SOX11 direct target genes that may explain the relationship between SOX11 and tumor microenvironment protective interactions to find new

Submitted 5 April 2017; accepted 16 May 2017. Prepublished online as *Blood* First Edition paper, 22 May 2017; DOI 10.1182/blood-2017-04-776740.

*P.B. and J.P. contributed equally to this study.

The online version of the article contains a data supplement.

There is an Inside *Blood* Commentary on this article in this issue.

The publication costs of this article were defrayed in part by page charge payment. Therefore, and solely to indicate this fact, this article is hereby marked "advertisement" in accordance with 18 USC section 1734.

© 2017 by The American Society of Hematology

Downloaded from http://ashpublications.org/blood/article-pdf/130/4/501/1404829/blood776740.pdf by guest on 23 April 2024

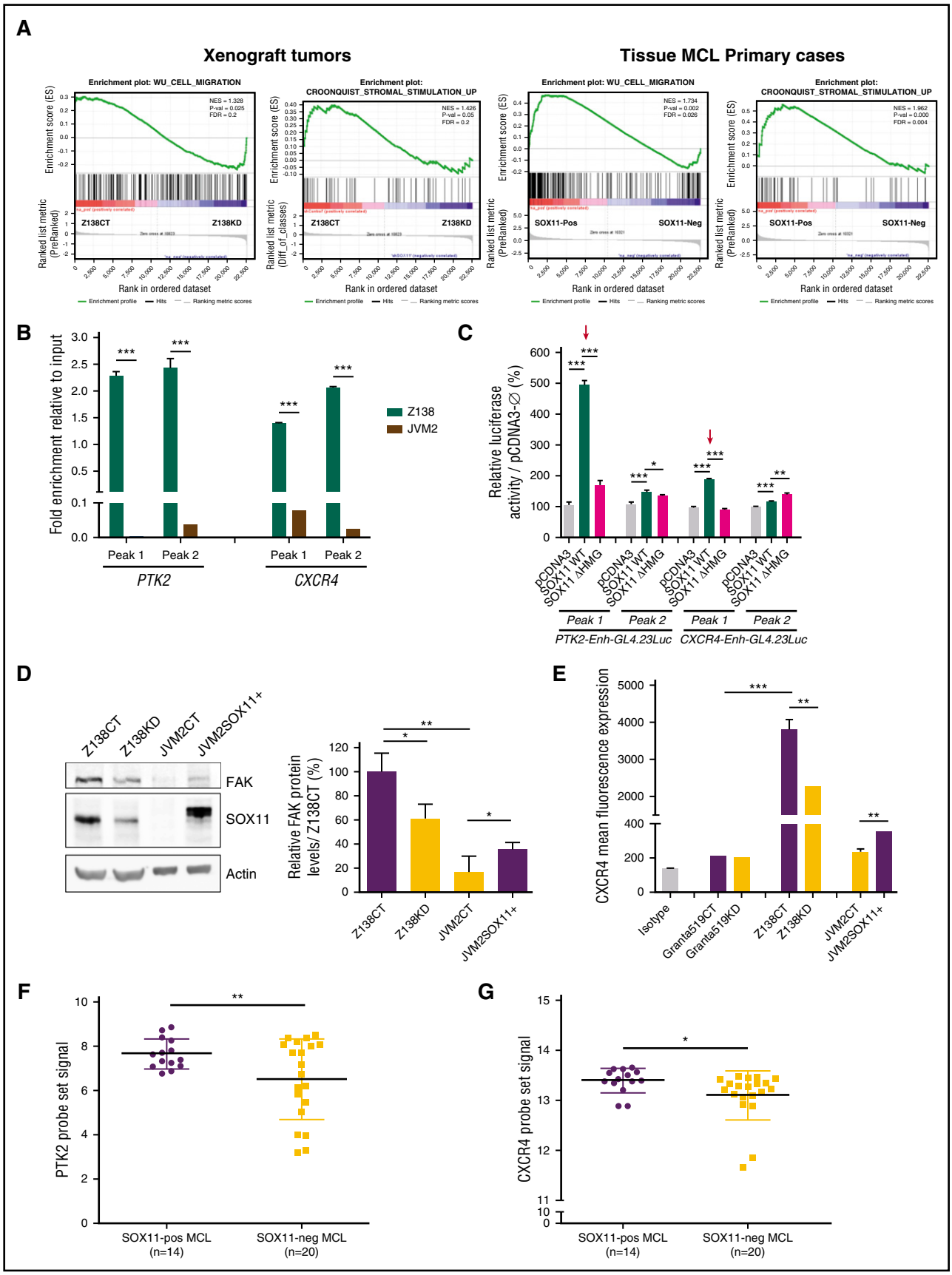

Figure 1. SOX11 directly regulates *CXCR4* and *PTK2* gene expression. (A) GSEA analysis on gene expression profiling microarray data from SOX11$^+$ (Z138CT) and SOX11KD (Z138KD) xenograft tumors and tissue SOX11$^+$ and SOX11$^-$ MCL primary cases, using microenvironment-related gene sets described in "Methods." Normalized enrichment score (NES), *P* value, and false-discovery rate (FDR) are shown. FDR <0.2 indicates statistical significance. (B) ChIP-qPCR enrichment in Z138 and JVM2 MCL

Downloaded from http://ashpublications.org/blood/article-pdf/130/4/501/1404829/blood776740.pdf by guest on 23 April 2024

potential targets for novel therapeutic strategies to prevent chemotherapy refractoriness in patients with aggressive MCL.

Methods

Cell lines and primary tumors

Two well-characterized SOX11$^+$ MCL cell lines (Z138 and Granta519) were used for SOX11-silencing (Z138 knockdown [KD] and Granta519KD, respectively).[11] In addition, the SOX11$^-$ MCL cell line (JVM2) and the chronic lymphocytic leukemia (CLL) cell line (JVM13) were used for FLAG-tagged SOX11 ectopical expression by stable lentiviral transduction (JVM2SOX11$^+$ and JVM13SOX11$^+$; supplemental Methods, available on the *Blood* Web site). All these cells were used for western blot, chromatin immunoprecipitation quantitative polymerase chain reaction (ChIP-qPCR), in vitro experiments, and/or immunohistochemical studies. Z138CTLuci and Z138KDLuci, obtained by stable lentiviral transduction expressing the luciferase enzyme[22] (supplemental Methods) from Z138CT and Z138KD cell lines,[11] respectively, were used for in vivo experiments. Human embryonic kidney 293T (HEK293T) cells were used for luciferase assays and lentiviral particle production. Human umbilical vein endothelial cells (HUVECs) were used for in vitro transmigration experimental studies. The BM mesenchymal cell line SNKT[23] expressing green fluorescent protein (SNKT-GFP$^+$; supplemental Methods) was used for coculture in in vitro system experiments.

Highly purified tumor cells (>95%) from 9 primary MCLs (5 SOX11$^+$ and 4 SOX11$^-$) were used for in vitro experiments (supplemental Table 1). Details on cell culture and human primary tumor information are provided in supplemental Methods.

Gene expression profiling and GSEA analyses

To identify oncogenic pathways related to SOX11 expression in MCL, we performed gene set enrichment analysis (GSEA) on gene expression data sets derived from SOX11$^+$ vs SOX11$^-$ MCL primary tumors (GSE21452),[24] SOX11$^+$ and SOX11KD MCL xenograft tumors (GSE52892),[12] and ChIP-chip data (GSE3502).[11] Experimental details on GSEA information are provided in supplemental Methods.

ChIP-qPCR

In vitro SOX11 binding to *CXCR4* and *PTK2* regulatory regions was identified by SOX11-specific ChIP-chip experiments[11] (supplemental Figure 1) and validated in Z138 and JVM2 MCL cell lines by ChIP-qPCR using specific primers (supplemental Table 2) as previously described[12] (supplemental Methods).

Luciferase assay

pGLA4.23-*CXCR4* and pGLA4.23-*PTK2* reporter constructs (supplemental Figure 1) were generated by PCR using specific primers (supplemental Table 2). Reporter constructs in cotransfections with SOX11 full-length (pcDNA3-HA-SOX11) or the truncated SOX11 protein (pcDNA3-HA-SOX11ΔHMG) expression vectors[11] were used for luciferase assay experiments, performed as previously described[12] (supplemental Methods).

Western blot and FC analyses

Protein extract preparation and western blot analysis were performed as previously described.[12] Primary antibodies used were SOX11 (MRQ-58; Cell Marque), phosphorylated FAKY397 (p-FAK; Cell Signaling Technology), FAK (32855; Cell Signaling), p-AKT S473 (Cell Signaling), AKT (sc-1618; Santa Cruz Biotechnology), p-MAPK T202/Y204 (p-ERK; 42/44; Cell Signaling), ERK1/2 (sc-94; Santa Cruz Biotechnology), and β-actin (Sigma). Flow cytometry (FC) analyses were performed as previously described.[11] Primary antibodies used were CXCR4 (anti-CD184 antibody; clone 12G5; BD Biosciences) conjugated with phycoerythrin (PE), p-AKT S473 (Cell Signaling) and p-MAPK T202/Y204 (p-ERK; 42/44; Cell Signaling) with the secondary antibody Alexa Fluor 488 dye (Life Technologies; supplemental Methods).

In vitro inhibition experiments and BZM treatments

MCL cells were pretreated with 10 μM of FAK inhibitor PF-573228 (PF)[25,26] for 6 hours, with 40 μM of CXCR4 antagonist AMD3100 octahydrochloride hydrate (AMD)[27] for 1 hour (both from Sigma-Aldrich) or with 1 μM of idelalisib (IDEL)[28] for 1 hour (Selleck Chemicals). Preteated MCL cells were washed 1 time with phosphate-buffered saline (PBS) and treated with 10 nM of bortezomib (BZM[29]; Janssen Pharmaceuticals) during 24 hours, when indicated.

CXCL12- or CXCL13-mediated chemotaxis

A total of 0.5×10^5 MCL cells in fetal bovine serum–free RPMI 1640 medium were added on top of a 24-well plate containing chambers with nontreated 5-μm pore size inserts (Corning Life Sciences) and transwells pretreated with 20 μg/mL of fibronectin (FN; Sigma) for 2 hours or preincubated overnight with 1×10^5 HUVECs. After overnight incubations, MCL-migrated cells toward CXCL12 200 ng/mL or CXCL13 1 μg/mL (both from Peprotech) were counted by FC in an Attune acoustic focusing cytometer (Life Technologies).

Pseudoemperipolesis, cell proliferation, and death analyses

MCL cells untreated or pretreated with AMD, PF, or IDEL were washed once with PBS and then added on top of a confluent SNKT-GFP$^+$ cell layer (1:5 SNKT/MCL ratio in case of MCL cell lines or 1:10 for MCL primary samples). MCL cells that had migrated to the SNKT-GFP$^+$ layer were distinguished by GFP$^-$ gating and cell size and counted by FC. MCL proliferation was determined by FC every day up to 3 days of coculture with SNKT-GFP$^+$ cells. To analyze apoptosis, MCL cells growing alone or in coculture with SNKT-GFP$^+$ cells and treated with 10 nM of BZM were labeled with Annexin V-PE (eBioscience), and cell death was analyzed by FC.

In vivo MCL cell migration and engraftment assays in xenograft mice models

With the use of a protocol approved by the animal testing ethical committee of the University of Barcelona, CB17 severe combined immunodeficient (SCID) mice (Janvier LABS, France) were intravenously (iv) inoculated into their tail veins with Z138CTLuci or Z138KDLuci cells, 10×10^6 cells per mouse and 8 mice in each group, generating SOX11$^+$ and SOX11KD xenograft mouse models (Z138CT and Z138KD, respectively). For in vivo inhibitory experiments, Z138CTLuci cells were preincubated with 10 μM of PF for 6 hours or 40 μM of AMD for 1 hour before being iv inoculated into SCID mice. Then, Z138CT mice were treated every day for 28 days with 30 mg/kg of PF,[30] 10 mg/kg of AMD,[31] or PBS as a control. Tumor dissemination and growth in Z138CT and Z138KD mice were captured by

Figure 1 (continued) cell lines of the SOX11 pulldown in *CXCR4* and *PTK2* loci (peak 1 and peak 2; supplemental Figure 1). DNA enrichment is displayed as fold change relative to their respective input chromatin. (C) Luciferase assays in transient cotransfections of *CXCR4* and *PTK2* enhancer GL4.23Luc (peak 1 and peak 2) with full-length SOX11 (pcDNA3SOX11) and truncated SOX11 (pcDNA3 ΔHMGSOX11) in HEK293T cell line. Results are shown as percentage fold induction referred to luciferase activity in cotransfection with the empty vector (pcDNA3-Ø). Red arrows indicate the most significant activated enhancers by SOX11 expression. (D) Western blot experiments showing total cellular FAK and SOX11 protein levels in Z138CT, Z138KD, JVM2CT, and JVM2SOX11$^+$ MCL cell line models ("Methods"). Notice that the slight band shift of SOX11 in JVM2SOX11$^+$ is a result of its expression with a FLAG tag. Actin was used as a loading control (left). Bar graph representing fold change differences in percentage of FAK protein levels in MCL cell lines, corrected by quantification of actin expression levels. Relative fold enrichment is displayed in reference to FAK protein levels of the SOX11$^+$ Z138CT cell line (right). (E) Bar graph representing the mean fluorescence of FC experiments showing the expression levels of cellular surface CXCR4 protein levels in Granta519 and Z138CT vs its KD counterparts and JVM2SOX11$^+$ vs JVM2CT MCL cell lines. Granta519 was used as a CXCR4$^-$ control cell line. Isotype immunoglobulin G control antibody was used as a negative CXCR4 control staining. Average levels of the *PTK2* (F) and *CXCR4* (G) probe set signals obtained from the analysis of Affymetrix HG-U133 2.0 plus microarrays from our 34 PB primary MCL tumors (14 SOX11$^+$ and 20 SOX11$^-$). Bar plot represents the mean percentage ± standard deviation of 3 independent experiments. The significance of difference was determined by independent samples Student *t* test: $^*P < .05$, $^{**}P < .01$, $^{***}P < .001$. WT, wild type.

Downloaded from http://ashpublications.org/blood/article-pdf/130/4/501/1404829/blood776740.pdf by guest on 23 April 2024

luciferase bioimage (LBI) once a week for 4 weeks. Mice were euthanized at 24 hours for the in vivo migration and 28 days postinoculation (PI) for MCL FC analysis. The number of MCL cells was determined by FC analysis using a specific anti-human CD19-PE antibody (Miltenyi Biotec) in PB, lymph nodes (LNs), BM, and spleen. Percentage of recovered MCL cells was normalized to the total number of cells in each specific tissue analyzed and the total number of injected cells. Details on mice in vivo experiments are provided in supplemental Methods.

Statistical analysis

Data are represented as mean ± standard deviation of 3 independent experiments. Statistical tests were performed using GraphPad Prism 5 software. Comparison between 2 groups of samples was evaluated by independent sample Student *t* test, and results were considered statistically significant when $P < .05$.

Results

SOX11 directly controls *CXCR4* and *PTK2* gene expression in MCL

To test the hypothesis that SOX11 could play a relevant role in MCL tumor microenvironment interactions, we revisited our gene expression profiling and ChIP-chip data on MCL tumors. Reanalysis of differentially expressed genes by GSEA showed that SOX11$^+$ xenograft tumors[12] and primary MCLs,[24] compared with their SOX11$^-$ counterparts, were significantly enriched in cell migration and stromal stimulation signatures (Figure 1A). Integrating GSEA data with SOX11-specific ChIP-chip data,[11] we found *CXCR4* and *PTK2* genes (encoding for FAK) to be the most significant SOX11-specific direct target genes within these tumor microenvironment pathways.

We validated the binding of SOX11 to the corresponding *CXCR4* and *PTK2* regulatory regions, showing significant fold enrichment of *CXCR4* and *PTK2* loci in the ChIP-qPCR experiments in Z138-DNA compared with JVM2-DNA using a specific SOX11 antibody over their inputs (Figure 1B; supplemental Figure 1A-C). Significant luciferase activity induction was detected in the coexpression of *CXCR4* and *PTK2* luciferase reporters with SOX11, predominantly at peak 1 of both genes, but not with SOX11 protein lacking the HMG domain (ΔHMGSOX11), which is required for its transcriptional activity (Figure 1C). Next, we analyzed CXCR4 and FAK protein levels in the Z138 MCL cell line upon SOX11 silencing (Z138KD)[11] and in the SOX11$^-$ JVM2 MCL cell line (JVM2CT) stably transduced for FLAG-SOX11 expression (JVM2SOX11$^+$). FAK and CXCR4 protein levels were higher in SOX11$^+$ MCL cells (Z138CT and JVM2SOX11$^+$) compared with their SOX11$^-$ counterparts (Z138KD and JVM2CT, respectively; Figure 1D-E). SOX11-regulating FAK and CXCR4 protein expression was validated in the JVM13 CLL cell line stably transduced for FLAG-SOX11 expression (JVM13SOX11$^+$), which expressed higher levels of these 2 proteins compared with the JVM13CT cell line (supplemental Figure 2A-B). Accordingly, messenger RNA quantification in human MCL primary tumors[9] showed significantly higher *PTK2* and *CXCR4* messenger RNA levels in SOX11$^+$ compared with SOX11$^-$ MCL cells (Figure 1F-G). Together these results suggest the direct transcriptional regulation of *CXCR4* and *PTK2* by SOX11 in MCL.

SOX11 promotes in vitro cell migration through the activation of the CXCR4 and FAK signaling pathways

To determine the role of SOX11 in MCL cell migration in a CXCR4- and FAK-dependent manner,[32-34] we first tested whether the expression of SOX11 affects CXCL12- and CXCL13-mediated chemotaxis of our MCL cell lines in in vitro models. In comparison with SOX11$^-$ cells (Z138KD and JVM2CT), SOX11-expressing cells (Z138CT and JVM2SOX11$^+$, respectively) displayed higher chemotaxis indices only toward CXCL12 but not toward CXCL13, through noncoated (supplemental Figure 3) or FN-coated transwells (Figure 2A), as well as higher transendothelial migration through HUVEC-coated transwells (Figure 2B). These results suggest that SOX11-induced MCL cell migration is largely dependent on the CXCR4/CXCL12 axis.

In in vitro inhibitory experiments, we observed that the CXCR4 antagonist (AMD)[27] inhibited CXCL12-mediated chemotaxis and transendothelial migration in both SOX11$^+$ and SOX11$^-$ MCL cell lines. On the contrary, the FAK inhibitor (PF)[25] only decreased chemotaxis and transendothelial migration in SOX11$^+$ but not in SOX11$^-$ MCL cells (Figure 2A-B). MCL cell proliferation and viability were not affected by either of these 2 compounds under same dosage and time conditions (supplemental Table 3). Same results were obtained in JVM13CT vs JVM13SOX11$^+$ CLL cell chemotaxis (supplemental Figure 4). Consistent with chemotaxis experiments, actin polymerization was impaired upon SOX11 KD in the Z138 MCL cell line (Z138KD) or when SOX11$^+$ (Z138CT) MCL cells were pretreated with AMD or PF (supplemental Figure 5). SOX11 expression also promoted CXCL12-mediated chemotaxis through FN-coated and HUVEC-coated transwells in human MCL primary tumor cells (Figure 2C-D, respectively). Moreover, the treatment with CXCR4 and FAK inhibitors eliminated differences in cell migration between SOX11$^+$ and SOX11$^-$ MCL primary tumor cells (Figure 2C). These results suggest a critical role of FAK in SOX11-induced MCL cell migration and show that SOX11 together with other factors may contribute to CXCR4/CXCL12-mediated chemotaxis in MCL.

SOX11 promotes crosstalk between MCL cells and stromal cells through the activation of the CXCR4 and FAK signaling pathways

To elucidate the role of SOX11 in promoting crosstalk between MCL and stromal cells, we studied spontaneous migration of our MCL cells beneath stromal cells (pseudoemperipolesis).[35] We observed that cocultures between MCL cells and the CXCL12-secreting BM stromal-cell line (SNKT) induced higher SOX11$^+$ tumor-cell migration beneath SNKT cells compared with SOX11$^-$ MCL counterpart cells, both in our MCL cell line models and primary tumor cells. Interestingly, both PF and AMD treatments blocked pseudoemperipolesis in SOX11$^+$ but not in SOX11$^-$ MCL cells (Figure 3A-B). Similar results were observed in JVM13CT vs JVM13SOX11$^+$ cell lines (supplemental Figure 6). These results suggest that contact between MCL cells and stromal cells mediated by SOX11 expression is dependent on FAK and the CXCR4/CXCL12 axis. Intriguingly, coculture between MCL cells and stromal cells induced the expression of CXCR4 in the tumor cells independently of SOX11 expression (Figure 3C), suggesting that additional microenvironmental factors may influence CXCR4 expression in MCL. Previous studies in hematopoietic progenitors have shown that the CXCR4/CXCL12 axis induces FAK activation.[36] Accordingly, we observed that recombinant CXCL12 induced p-FAK at Y397 in SOX11$^+$ MCL cell lines without increasing total FAK (Figure 3D). Moreover, coculture between MCL cells and stromal cells also induced p-FAK in SOX11$^+$ but not in SOX11$^-$ MCL cells (Figure 3E; supplemental Figure 7A).

Together, these results suggest that SOX11 stimulates CXCR4 and FAK expression in MCL cells. Contact between MCL cells and CXCL12-secreting stromal cells reinforces p-FAK in the neoplastic cells, inducing migration and strong adhesion of the MCL cells beneath the stromal cells in a SOX-dependent manner. AMD and PF can block pseudoemperipolesis in SOX11$^+$ MCL cells, suggesting that their migration and adhesion depend on the CXCR4/FAK axis.

Downloaded from http://ashpublications.org/blood/article-pdf/130/4/501/1404829/blood776740.pdf by guest on 23 April 2024

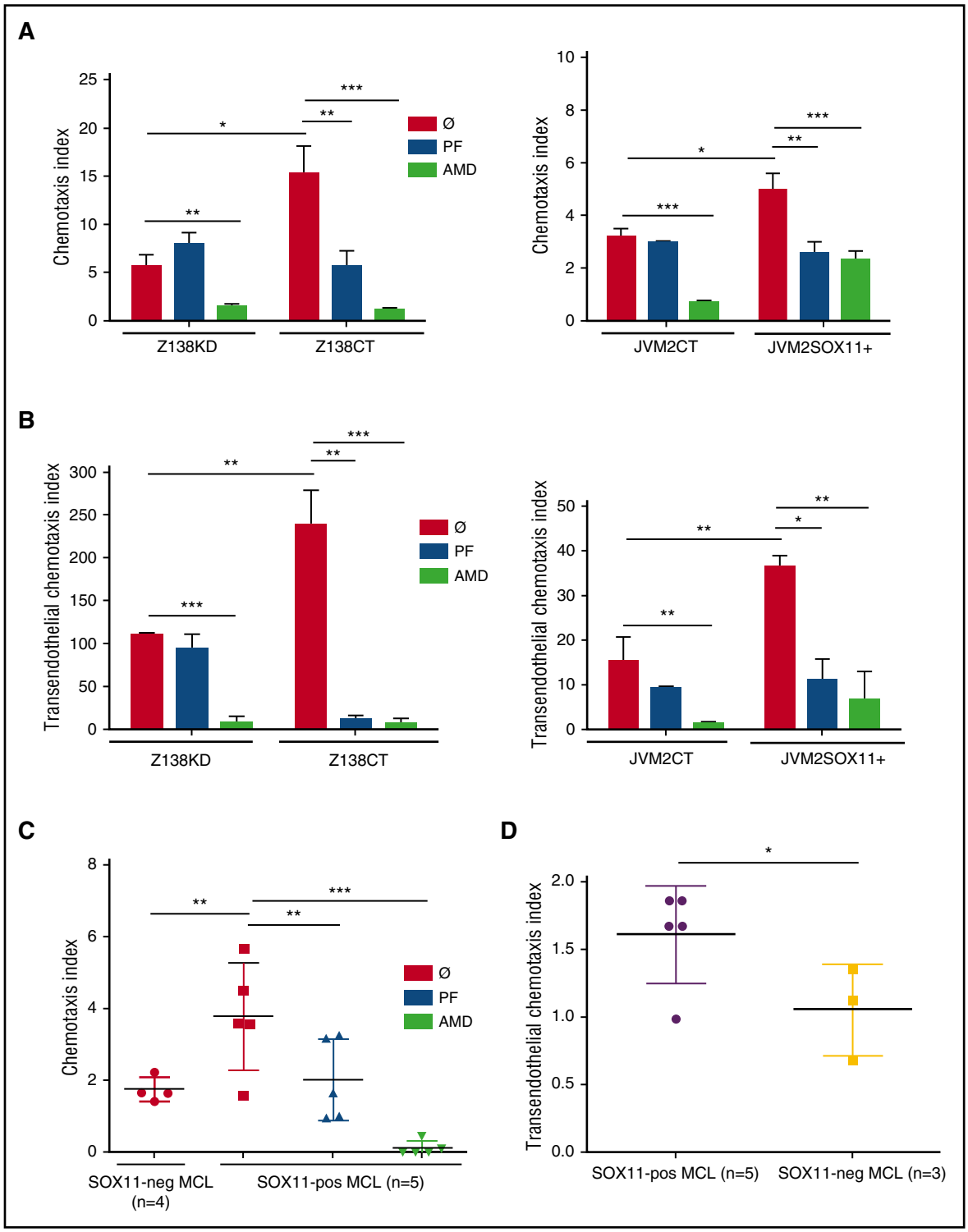

Figure 2. SOX11 promotes in vitro CXCL12-mediated chemotaxis through CXCR4/FAK signaling activation in MCL. (A-B) 5×10^5 SOX11$^+$ MCL cells in in vitro models (Z138CT and JVM2SOX11$^+$) and their SOX11$^-$ counterparts (Z138KD and JVM2CT MCL cell lines, respectively) untreated (Ø) or pretreated for 6 hours with 10 μM of specific FAK inhibitor (PF) or for 1 hour with 40 μM of the CXCR4 antagonist (AMD) were seeded in the upper chamber of FN-coated transwells (A) or transwells coated with HUVEC cells (B). After overnight incubation, Z138CT- and Z138KD-migrated (left) and JVM2SOX11$^+$ and JVM2CT-migrated (right) cells toward recombinant CXCL12 at the bottom chamber of the transwells were quantified by FC. (C) Same CXCL12-mediated chemotaxis assays as in panel A were performed using MCL cells derived from PB (>95% purified) of human primary MCL (5 SOX11$^+$ and 4 SOX11$^-$ MCL primary cells). (D) 5×10^5 MCL cells from MCL primary tumors (5 SOX11$^+$ and 3 SOX11$^-$ MCL cases) were seeded on the upper chamber of transwells coated with HUVEC cells. After overnight incubation, migrated cells toward recombinant CXCL12 at the bottom chamber of the transwell were quantified by FC. Migration index was calculated as number of MCL cells that migrated in the presence of the chemoattractant (CXCL12-dependent migration) divided by the number of migrated cells in the absence of the chemokine (unspecific migration). Bar plot represents the mean percentage ± standard deviation of 3 independent experiments. The significance of difference was determined by independent samples Student *t* test: **P* < .05, ***P* < .01, ****P* < .001.

Downloaded from http://ashpublications.org/blood/article-pdf/130/4/501/1404829/blood776740.pdf by guest on 23 April 2024

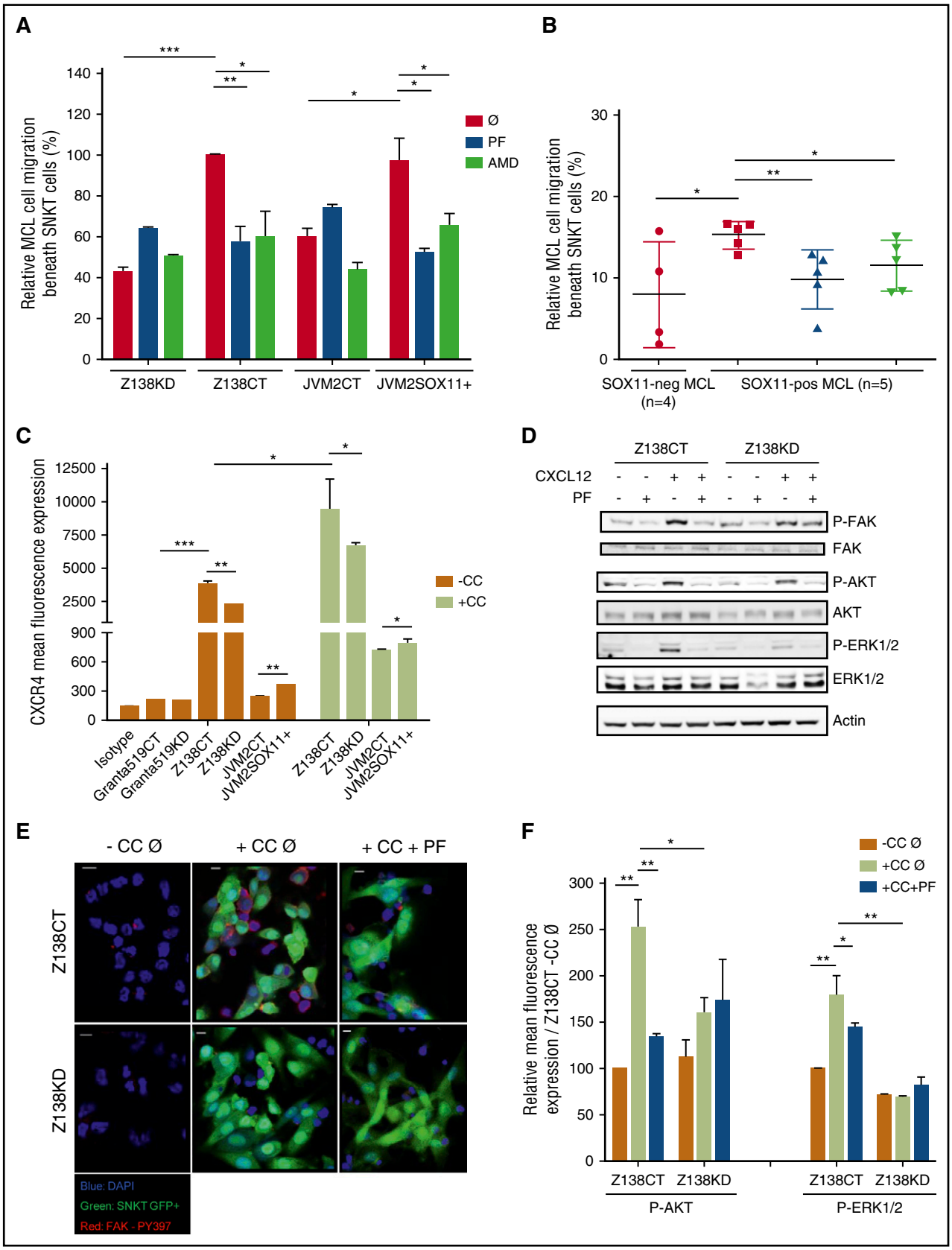

Figure 3. SOX11 expression promotes pseudoemperipolesis through CXCR4 and FAK pathway activation in MCL. First we analyzed SOX11-dependent MCL cell migration beneath SNKT cells (pseudoemperipolesis). (A) SOX11$^+$ and SOX11$^-$ in vitro MCL cell line models untreated (Ø) or treated with PF or AMD were added to SNKT-GFP$^+$ layers or (B) SOX11$^+$ MCL cells derived from PB (>95% purified) of primary MCLs (n = 5) untreated (Ø) or pretreated with PF or AMD and untreated cells derived from SOX11$^-$ (n = 4) MCL primary samples were cocultured with SNKT-GFP$^+$ cells. After overnight incubations, cocultures described in panels A and B were washed several times, and MCL cells that had migrated toward the stromal layer were trypsinized and counted by FC; MCL cells were distinguished by GFP$^-$ gating and cell size. Results in

Downloaded from http://ashpublications.org/blood/article-pdf/130/4/501/1404829/blood776740.pdf by guest on 23 April 2024

SOX11/FAK/ERK axis promotes stromal microenvironment–mediated MCL cell proliferation

FAK activation demonstrated by phosphorylation at Y397 (p-FAK) can stimulate several downstream signaling pathways to promote tumor-cell survival and proliferation, including PI3K/AKT and ERK1/2 pathways.[26,37-39] Concordantly, we observed that recombinant CXCL12 or in vitro interactions with stromal cells increased FAK activation (p-FAK), causing downstream p-AKT and p-ERK in SOX11$^+$ but not, or at low levels, in SOX11KD MCL, whereas basal levels of these proteins did not change (Figure 3D-F; supplemental Figure 7A-B).

Accordingly, in in vitro cocultures, SOX11-expressing MCL cells acquired advantages in cell proliferation compared with the SOX11$^-$ MCL counterparts (Figure 4A), whereas no differences in proliferation were observed when they were cultured alone (data not shown).[11] We also observed that only direct contact between MCL and SNKT cells promoted rapid cell proliferation in Z138CT but not in Z138KD cells (Figure 4B). PF treatments impaired FAK activation and downstream p-AKT and p-ERK1/2 (Figure 3D-F; supplemental Figure 7A-B) and significantly inhibited tumor-cell proliferation in SOX11$^+$ but not in SOX11$^-$ MCL cell lines in contact with stromal cells (Figure 4A). Together, these results suggest that SOX11-increased FAK expression and its phosphorylation by chemokines or adhesion molecules activate downstream PI3K/AKT and ERK1/2 signaling pathways in MCL that promote stromal-cell contact–dependent MCL proliferation.

SOX11/FAK/PI3K axis mediates CAM-DR in MCL

Adhesion to stromal cells in microenvironment niches protects malignant B cells from apoptosis induced by drugs in a process called stromal CAM-DR.[14] To determine the role of SOX11 expression in CAM-DR, we analyzed BZM-induced cell death in SOX11$^+$ and SOX11$^-$ MCL cells in cocultures with vs without the SNKT-BM stromal-cell line. We observed that SOX11$^+$ MCL cell lines and primary tumor cells in coculture with SNKT were more protected from BZM-induced cell death than their SOX11$^-$ counterparts (Figure 5A-B). Moreover, we observed that only in coculture conditions, but not in MCL monocultures, did PF or AMD in combination with BZM treatment significantly increase MCL cell death compared with individual BZM treatment (supplemental Figure 8A-B). The protective effect of SNKT cells was reduced after specific inhibition of FAK only in SOX11$^+$ MCL cell lines and primary MCL cases, with survival levels similar to those of their SOX11$^-$ counterparts (Figure 5A-B). Additionally, a specific PI3K inhibitor, IDEL, overcame SOX11-mediated CAM-DR to BZM in SOX11$^+$ but not in SOX11$^-$ MCL cells, with inhibitory effects similar to those obtained with PF pretreatments (Figure 5A). Together, these results reinforce the idea that close contact between MCL and stromal cells is required for CAM-DR in MCL and that this is mediated by SOX11 through the activation of the FAK/PI3K signaling pathway.

FAK- and CXCR4-specific inhibitors block in vivo SOX11-induced MCL cell homing and engraftment in intravenous xenograft mouse models

To test whether SOX11 expression in MCL affects migration and invasion in vivo, 10 million SOX11$^+$ and SOX11$^-$ Z138 MCL cells stably transduced to express the luciferase enzyme (Z138CTLuci and Z138KDLuci, respectively) were injected iv into immune-depressed SCID mice.

First, we analyzed in vivo MCL cell migration 24 hours PI. We observed a significantly higher number of MCL cells recovered from BM of Z138CT compared with Z138KD mice (Figure 6A; supplemental Figure 9), suggesting that SOX11 expression promotes MCL cell migration to BM in vivo. Then, tumor engraftment was monitored every week by LBI.[31] LBI signals in BM and LNs were already detected in a majority of the Z138CT mice 2 to 3 weeks PI, whereas in Z138KD mice, LBI signals were undetectable until week 4 PI, showing significant differences at the final time (Figure 6B-C; supplemental Figure 10A-B). Accordingly, 28 days PI, a significantly higher number of MCL cells were recovered from BM and LNs of Z138CT compared with Z138KD mice, whereas no differences were observed in spleen (supplemental Figure 9C). On the contrary, we found a significantly lower number of MCL cells in PB of Z138CT compared with Z138KD mice (Figure 6D; supplemental Figure 9C), suggesting that SOX11KD impairs MCL cell migration to BM and LNs.

At day 40 PI, some Z138KD mice presented high LBI signals, similar to those of Z138CT. However, immunohistological analysis showed that these BM Z138KD tumors were mainly composed of SOX11$^+$ cells, suggesting that the subset of SOX11$^+$ cells remaining in the Z138KD pool, because the silencing is not 100% (Figure 1D), may take over and grow in the BM and LNs after prolonged periods (data not shown).

To confirm the role of CXCR4 and FAK in SOX11-mediated MCL dissemination in vivo, we treated Z138CT mice with AMD and PF, which significantly reduced tumor dissemination and growth to the same levels as in Z138KD mice (Figure 6B-C). Concordantly, we found a significant decrease in the number of MCL cells recovered from BM of Z138CT-treated mice, reaching numbers similar to those in Z138KD mice. The number of MCL cells recovered from LNs in Z138CT mice significantly decreased only when they were treated with PF but not with AMD, suggesting that the CXCR4/CXCL12 axis plays a critical role in the homing of MCL cells toward BM, whereas other factors may play a role in attraction toward LNs in in vivo xenograft MCL models. Moreover, Z138CT mice treated with AMD or PF displayed higher numbers of MCL cells in PB than control mice treated with vehicle PBS and similar numbers to those of MCL cells recovered from the PB of Z138KD mice (Figure 6D). Together, our in vivo results suggest that the SOX11/CXCR4/FAK axis plays an important role in MCL tumorigenesis, promoting in vivo organ dissemination and

Figure 3 (continued) panel A are shown as relative to the corresponding untreated SOX11$^+$ MCL cell line (Z138CTØ and JVM2SOX11Ø, respectively). (C) Bar graph representing the mean fluorescence of FC experiments showing the expression levels of cellular surface CXCR4 protein levels in Granta519 and Z138CT vs their KD MCL cell lines counterparts, and JVM2SOX11$^+$ vs JVM2CT MCL cell lines growing alone (−CC) or in coculture with the human BM stromal-cell line (SNKT; +CC). Granta519 was used as a CXCR4$^-$ control cell line. Isotype immunoglobulin G control antibody was used as a negative CXCR4 control staining. (D) Western blot experiments showing expression levels of basal forms of FAK, AKT, and ERK1/2 proteins and p-FAK, p-AKT, and p-ERK in Z138CT and Z138KD pretreated with PBS (−) or with PF (+) and cultured 30 minutes in RPMI plus 10% fetal bovine serum with PBS (−) or with CXCL12 (+). Actin was used as a loading control. (E) FAK Tyr^{397} phosphorylation was determined by confocal microscopy. Z138CT and Z138KD cells untreated (Ø) or pretreated with PF (+PF) were seeded over covered glasses growing alone (−CC) or in coculture with SNKT-GFP$^+$ layers (green cells; +CC). After overnight incubation, nonadhered cells were removed by several washes. Adhered cells above covered glasses were fixed, permeabilized, and labeled with a specific rabbit anti-Tyr^{397} p-FAK primary antibody and with PE secondary antibody (red signals). 4′,6-diamidino-2-phenylindole (DAPI) was used to determine cellular nuclei (blue cell nuclei). Bar, 10 μm. (F) Bar graph representing the mean fluorescence of FC experiments showing expression levels of p-AKT and p-ERK1/2 proteins in Z138CT and Z138KD cultured overnight alone (−CC) or in cocultures with SNKT-GFP$^+$ cells (+CC) and pretreated with PBS (Ø) or with the FAK inhibitor (+PF). Results are shown as mean fluorescence expression relative to Z138CT cultured overnight alone and pretreated with PBS (Z138CT −CC Ø). Bar plot represents the mean percentage ± standard deviation of 3 independent experiments. The significance of difference was determined by independent samples Student *t* test: $^*P < .05$, $^{**}P < .01$, $^{***}P < .001$.

Downloaded from http://ashpublications.org/blood/article-pdf/130/4/501/1404829/blood776740.pdf by guest on 23 April 2024

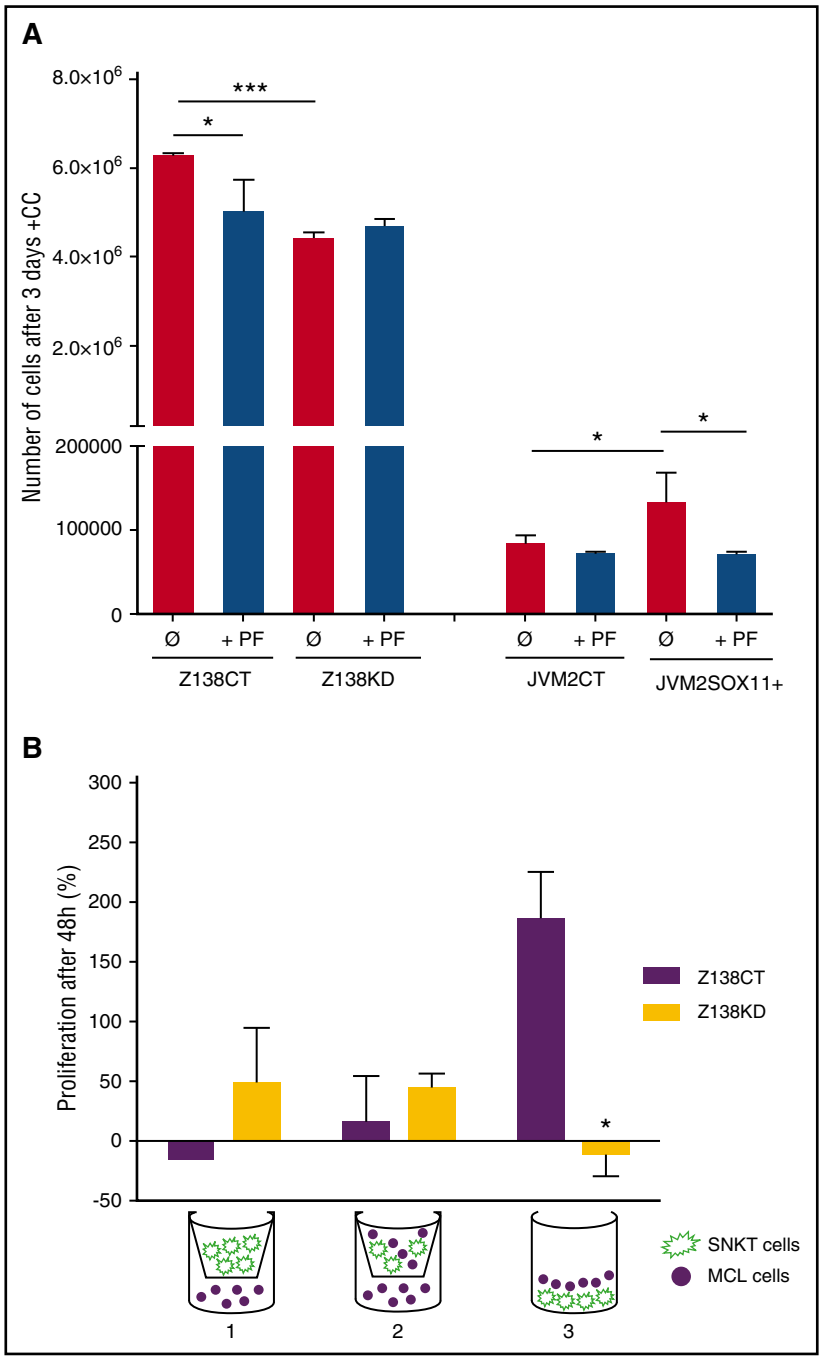

Figure 4. SOX11/FAK axis promotes proliferation of MCL in contact with marrow stromal cells. (A) Z138CT, Z138KD, JVM2CT, and JVM2SOX11$^+$ MCL cell lines untreated (Ø) or pretreated with PF were cocultured with BM stromal SNKT-GFP$^+$ cells. The number of MCL cells was counted by FC after 3 days of coculture. (B) Z138CT and Z138KD MCL cells (solid circle) were seeded in a 5:1 ratio: (1) with SNKT-GFP$^+$ cells (shown in green) on a transwell insert, (2) with a coculture of SNKT-GFP$^+$ and MCL cells on the transwell insert, and (3) in direct coculture with SNKT-GFP$^+$ cells. The number of MCL cells was counted by FC after 48 hours of coculture. Values are represented as percentage of increment in the number of MCL cells relative to the number of cells at day 0. Bar plot represents the mean percentage ± standard deviation of 3 independent experiments. The significance of difference was determined by independent samples Student *t* test: $^*P < .05$, $^{***}P < .001$.

growth. Furthermore, CXCR4 antagonist and FAK inhibitors represent promising therapeutic strategies to block MCL dissemination by retaining or allowing the recirculation of the tumor cells from the protective BM and LN microenvironments to the PB, where MCL cells would be more easily targeted by conventional treatments, such as anti-CD20 or BZM.

Discussion

SOX11 is overexpressed in a majority of MCLs, and its expression has been associated with more aggressive behavior and worse outcome.[5,8,40] Patients with SOX11$^-$ MCL present with leukemic non-nodal disease, whereas SOX11$^+$ tumors involve LNs and have extensive extranodal infiltration.[3-6,41] This suggests a higher invasive capacity of the SOX11$^+$ MCL cells toward tissue niches that may critically contribute to MCL progression and resistance to treatment.[16,42] Concordantly, here we found that SOX11$^+$ MCL xenograft and human primary MCL are enriched in protective microenvironment-related signatures, compared with SOX11$^-$ tumors. We demonstrate that *CXCR4* and *PTK2* are the most significant target genes within these tumor microenvironment pathways directly regulated by SOX11.

Activation of CXCR4 expression by SOX11 has been previously described in mesenchymal stem cells.[43] Here, our results show that

Downloaded from http://ashpublications.org/blood/article-pdf/130/4/501/1404829/blood776740.pdf by guest on 23 April 2024

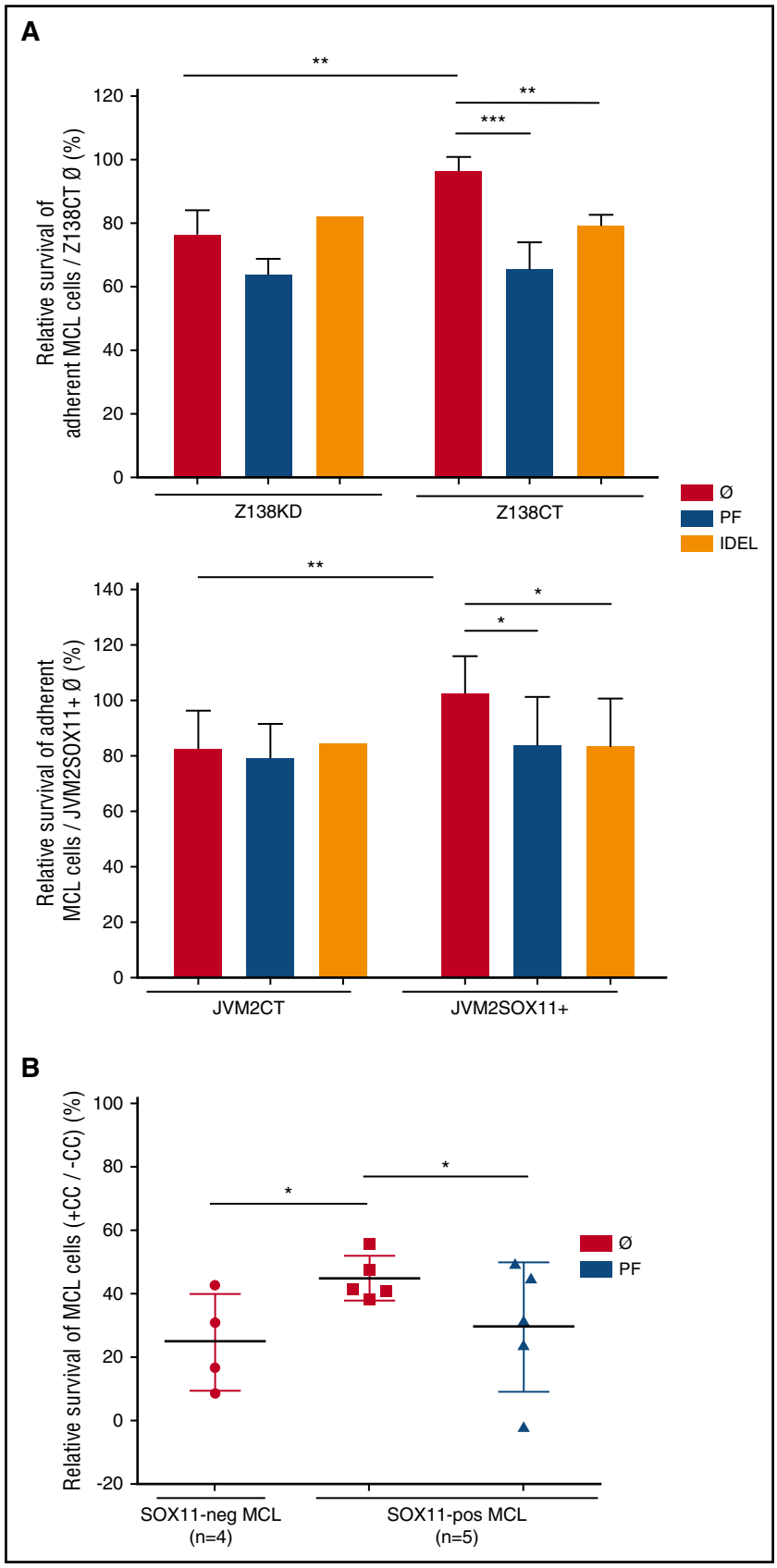

Figure 5. CAM-DR is regulated by SOX11 through activation of the FAK/PI3K signaling pathway. (A) Z138CT/Z138KD (upper) and JVM2SOX11$^+$/JVM2CT cells (lower), untreated (Ø) or pretreated with PF or IDEL, were seeded in coculture with stromal SNKT-GFP$^+$ cells and incubated with BZM. After overnight coculture and BZM incubation, adherent MCL cells were labeled with Annexin V-PE and analyzed by FC. MCL cells were distinguished by GFP$^-$ gating and cell size. Bar graphs correspond to the relative percentage of MCL cells cocultured with SNKTs that survived (Annexin V$^-$ cells) relative to the corresponding SOX11$^+$ untreated Annexin V$^-$ MCL cells (Z138CTØ or JVM2SOX11$^+$Ø, respectively). (B) SOX11$^+$ MCL cells derived from PB (>95% purified) of primary MCLs (n = 5) untreated (Ø) or pretreated with PF and untreated SOX11$^-$ (n = 4) MCL cells derived from primary MCL samples were seeded alone (−CC) or in coculture with stromal SNKT-GFP$^+$ cells (+CC) and then incubated with BZM for 24 hours. The pool (supernatant and adhered) of MCL cells was labeled with Annexin V-PE and analyzed by FC. Bar graphs correspond to the relative percentage of MCL cell cocultured with SNKTs (+CC) that survived (Annexin V$^-$ cells) relative to the corresponding Annexin V$^-$ MCL cells in −CC. Bar plot represents the mean percentage ± standard deviation of 3 independent experiments. The significance of difference was determined by independent samples Student *t* test: $^*P < .05$, $^{**}P < .01$, $^{***}P < .001$.

SOX11 directly binds to regulatory regions, promoting CXCR4 and FAK expression in MCL. FAK is a cytoplasmic nonreceptor tyrosine kinase activated by growth factor receptors or integrins that is essential in tumor microenvironment to facilitate cell migration,[44] invasion,[45] cancer progression, and metastasis.[33] Unlike solid tumors, the role of FAK in proliferation and dissemination of B-cell tumors is largely

Downloaded from http://ashpublications.org/blood/article-pdf/130/4/501/1404829/blood776740.pdf by guest on 23 April 2024

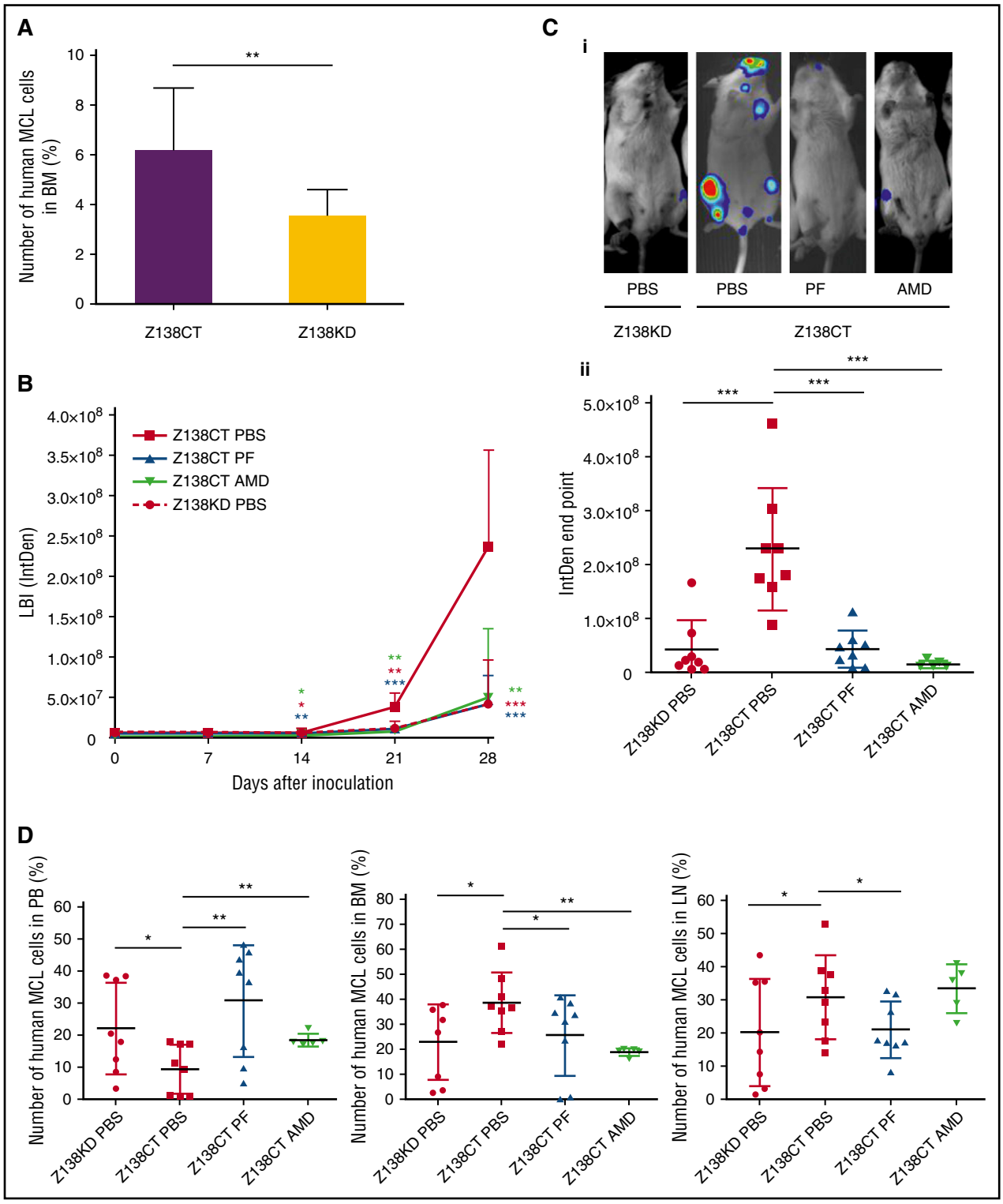

Figure 6. SOX11 expression promotes in vivo cell migration and specific BM and LN infiltration and engraftment through the activation of CXCR4 and FAK pathways in intravenous MCL xenograft models. Some 10×10^6 SOX11$^+$ and SOX11$^-$ Z138 MCL cell lines stably transfected to express a luciferase enzyme (Z138CTLuci and Z138KDLuci, respectively) were iv inoculated into SCID mice generating Z138CT and Z138KD mice, respectively. (A) In vivo MCL cell migration toward BM in Z138CT (n = 8) and Z138KD (n = 8) mice 24 hours PI was analyzed using a specific human anti-CD19–PE antibody to determine number of MCL cells in BM by FC. (B) Z138CT mice were randomly assigned and treated every day with 30 mg/kg PF (n = 8) or 10 mg/kg AMD (n = 6) for 28 days and compared with Z138CT and Z138KD control PBS-treated mice (n = 8 each). Graph showing tumor engraftment by quantification of the LBI signals (IntDen) at the indicated days PI. (C) Representative pictures showing MCL engraftment in nodal and extranodal sites 28 days PI by LBI signals of Z138CT mice intraperitoneally (ip) injected with vehicle PBS, PF, or AMD and Z138KD mice injected with vehicle PBS (i). Quantification of the LBI signals (IntDen) in individual Z138CT animals ip injected with vehicle PBS, PF, or AMD and Z138KD mice injected with vehicle PBS at day 28 PI (ii). (D) Graph displaying the number of recovered MCL cells (%) normalized to the total number of cells in PB, BM, and LNs, labeled with a specific human anti-CD19–PE antibody and analyzed by FC. The significance of difference was determined by independent samples Student *t* test: $^*P < .05$, $^{**}P < .01$, $^{***}P < .001$.

Downloaded from http://ashpublications.org/blood/article-pdf/130/4/501/1404829/blood776740.pdf by guest on 23 April 2024

unknown, although positive expression has been detected in several B-cell lymphomas, including MCL.[46]

Here, our in vivo experiments in mice receiving intravenous MCL xenotransplants demonstrate that SOX11$^+$ MCL cells display higher in vivo cell migration and invasion compared with the SOX11KD MCL cells. The delay of tumor onset in Z138KD mice and the higher number of MCL cells in BM and LNs in Z138CT mice also demonstrate that SOX11 expression provides advantages to MCL cells in crossing the endothelial vein barrier and invading nodal and extranodal tissues in vivo. On the contrary, SOX11KD impairs MCL cell tissue infiltration, retaining MCL cells in the blood stream. These results are consistent with the leukemic non-nodal clinical presentation of human primary SOX11$^-$ cells and highlight the implication of SOX11 in MCL dissemination, invasion, and aggressive progression.

Our in vitro results in MCL cell lines and primary patient cases confirm the role of CXCR4/CXCL12 axis in the homing of MCL cells.[14,19] Although additional microenvironmental factors seem to influence CXCR4 expression, its expression is further induced upon SOX11 upregulation, and the CXCR4/CXCL12 axis reinforces p-FAK at Y397[36] only in SOX11$^+$ MCL cell lines. Moreover, PF inhibits CXCL12-mediated cell migration in SOX11$^+$ but not in SOX11$^-$ MCL cell lines, suggesting that SOX11-mediated MCL cell migration is largely dependent on FAK, and the CXCR4/CXCL12 axis contributes to its activation in a SOX-dependent manner.

We observed that MCL cell adhesion and migration beneath the SNKT cells (pseudoemperipolesis) are higher in SOX11$^+$ compared with SOX11$^-$ cell lines. Moreover, PF and AMD reduced pseudoemperipolesis only in SOX11$^+$ MCL cells, achieving levels similar to those of their SOX11$^-$ counterparts. These results suggest that SOX11 plays a key role in the interactions and crosstalk between MCL cells and stromal cells through the activation of CXCR4 and FAK signaling pathways. In agreement with other cell models,[38,47] we observed that p-FAK at Y397 and activated ERK1/2 and PI3K/AKT downstream pathways increase in SOX11$^+$ MCL cells by CXCL12 stimulation or by its contact with SNKT cells, promoting MCL cell proliferation and survival.[26,37,38]

Contact between MCL cells and stromal cells protects MCL cells from BZM-induced cell death, a drug currently used in MCL therapy.[48,49] In coculture conditions, we observed that survival indices after BZM treatments were significantly higher in SOX11$^+$ compared with SOX11$^-$ MCL cells adhered to SNKT cells. These results suggest that SOX11 expression enhances the close contact and crosstalk of MCL cells with stromal cells, which in turn confer drug resistance and tumor-cell growth. Specific in vitro CAM-DR inhibition in SOX11$^+$ but not in SOX11$^-$ MCL cells by AMD, PF, and IDEL treatments reinforces the relevance of the SOX11/CXCR4/FAK/PI3K axis in human MCL pathogenesis.[21,50,51] Notably, our in vivo inhibitory experiments show that PF and AMD treatments significantly reduced the dissemination and development of SOX11$^+$ MCL in intravenous xenograft mouse models. We observed that engraftment reduction in SOX11$^+$ MCL mice is accompanied by a significant decrease of MCL cells in BM and LNs and a simultaneous increase of MCL cells in PB.

Overall, our results suggest a hypothetical model for the clinical and biological heterogeneity of SOX11$^+$ and SOX11$^-$ MCLs (Figure 7). SOX11 overexpression in MCL directly activates CXCR4 and FAK transcription. CXCR4 overexpression in SOX11$^+$ MCL cells and CXCL12 secreted by BM stromal cells enhance FAK activation, promoting MCL cell migration and adhesion to LNs and BM, facilitating crosstalk with the tissue stromal cells that confers survival and drug resistance signals to MCL cells. PI3K/AKT and ERK1/2 FAK-downstream pathways are activated in a SOX11-dependent manner, contributing to stromal-induced cell proliferation, survival, and drug resistance. Target inhibition of these pathways provides new strategies for disruption of the tumor-stromal protective interactions, facilitating the mobilization of MCL cells from their protective microenvironment to the PB and making them more accessible to conventional drugs, which may help to overcome minimal residual disease and relapse commonly seen in aggressive MCL.

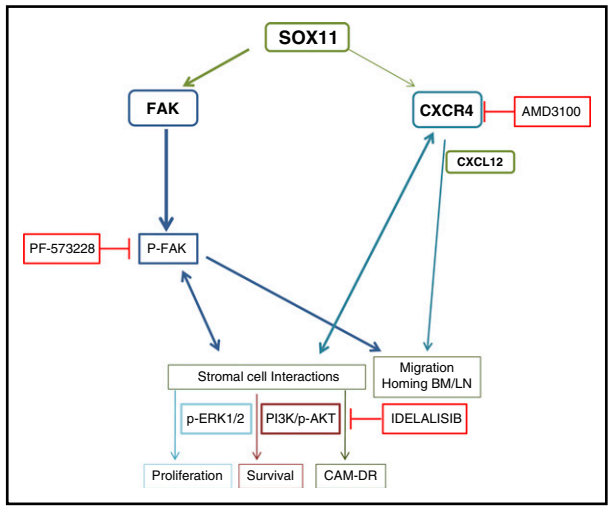

Figure 7. Hypothetical model for SOX11/CXCR4/FAK axis regulating MCL cell migration, crosstalk with the protective stromal microenvironment, progressive growth, and resistance to conventional treatments. SOX11 directly regulates CXCR4 and *PTK2*/FAK gene transcription, also influenced by tumor microenvironment factors. CXCR4 overexpression in SOX11$^+$ MCL cells and CXCL12 secretion by stromal cells at the tumor microenvironment enhance p-FAK at Y397, promoting MCL cell migration and adhesion to BM and LNs in a SOX11-dependent manner. The SOX11/CXCR4/FAK axis in MCL cells promotes crosstalk with BM stromal cells for protective microenvironment interactions through the activation of the PI3K/AKT and ERK1/2 FAK-downstream signaling pathways that contribute to stromal-induced cell proliferation, survival, and drug resistance (CAM-DR). Targeting FAK, CXCR4/CXCL12, and/or PI3K pathways could constitute new therapeutic strategies to disrupt the protective microenvironment interactions in relapsed/refractory aggressive MCL.

Acknowledgments

The authors thank the Hospital Clinic of Barcelona–Institut d'Investigacions Biomèdiques August Pi i Sunyer Biobank Tumor Bank and Hematopathology Collection for sample procurement and the Genomics Core Facility for technical help. This work was developed at the Centro Esther Koplowitz, Barcelona, Spain.

This work was supported by grants from the Ministerio de Economía y Competitividad (BFU2015-64879-R to V.A., SAF2015-64885-R to E.C., and SAF2014-57708-R to M.C.C.), Fundació La Marató de TV3 (TV3-Cancer-I3/20130110 to V.A.), Generalitat de Catalunya Suport Grups de Recerca (AGAUR 2014-SGR-2014 to V.A. and AGAUR 2014-SGR-795 to E.C.), and ISCIII project PIE13/00033, which is part of Plan Nacional de I+D+I and is cofinanced by the Subdirectorate General for Evaluation and the European Regional Development Fund (Fondo Europeo de Desarrollo Regional).

Authorship

Contribution: P.B. and J.P. performed all in vitro experiments; P.B. and M.L.R. performed all in vivo experiments; Á.E. and M.S.-G. performed luciferase assays; M.C.V. performed chromatin

Downloaded from http://ashpublications.org/blood/article-pdf/130/4/501/1404829/blood776740.pdf by guest on 23 April 2024

immunoprecipitation experiments; M.C.C. and E.P.-R. supervised the in vitro adhesion and migration experiments; E.C. identified mantle cell lymphoma tumors and analyzed data; V.A. designed, performed, and supervised experiments and analyzed data; P.B., V.A., E.C., and M.C.C. wrote the manuscript; and all authors discussed the results and commented on the manuscript.

Conflict-of-interest disclosure: The authors declare no competing financial interests.

ORCID profiles: P.B., 0000-0002-9485-9179; J.P., 0000-0002-2092-2526; Á.E., 0000-0002-0302-6762; M.C.V., 0000-0002-3165-1768; E.P.-R., 0000-0001-5948-2241; M.C.C., 0000-0002-4730-0938; E.C., 0000-0001-9850-9793; V.A., 0000-0002-3016-2874.

Correspondence: Virginia Amador, Centre Esther Koplowitz (CEK), C/ Rosselló 149-153, Barcelona 08036, Spain; e-mail: vamador@clinic.ub.es.

References

1. Swerdlow SH, Campo E, Harris NL, et al. WHO Classification of Tumours of Haematopoietic and Lymphoid Tissues. Lyon, France: IARC Press; 2008.
2. Swerdlow SH, Campo E, Pileri SA, et al. The 2016 revision of the World Health Organization classification of lymphoid neoplasms. *Blood*. 2016;127(20):2375-2390.
3. Espinet B, Ferrer A, Bellosillo B, et al. Distinction between asymptomatic monoclonal B-cell lymphocytosis with cyclin D1 overexpression and mantle cell lymphoma: from molecular profiling to flow cytometry. *Clin Cancer Res*. 2014;20(4):1007-1019.
4. Ondrejka SL, Lai R, Smith SD, Hsi ED. Indolent mantle cell leukemia: a clinicopathological variant characterized by isolated lymphocytosis, interstitial bone marrow involvement, kappa light chain restriction, and good prognosis. *Haematologica*. 2011;96(8):1121-1127.
5. Fernàndez V, Salamero O, Espinet B, et al. Genomic and gene expression profiling defines indolent forms of mantle cell lymphoma. *Cancer Res*. 2010;70(4):1408-1418.
6. Navarro A, Royo C, Hernández L, Jares P, Campo E. Molecular pathogenesis of mantle cell lymphoma: new perspectives and challenges with clinical implications. *Semin Hematol*. 2011;48(3):155-165.
7. Sander B, Quintanilla-Martinez L, Ott G, et al. Mantle cell lymphoma: a spectrum from indolent to aggressive disease. *Virchows Arch*. 2016;468(3):245-257.
8. Royo C, Navarro A, Clot G, et al. Non-nodal type of mantle cell lymphoma is a specific biological and clinical subgroup of the disease. *Leukemia*. 2012;26(8):1895-1898.
9. Navarro A, Clot G, Royo C, et al. Molecular subsets of mantle cell lymphoma defined by the IGHV mutational status and SOX11 expression have distinct biologic and clinical features. *Cancer Res*. 2012;72(20):5307-5316.
10. Jares P, Colomer D, Campo E. Molecular pathogenesis of mantle cell lymphoma. *J Clin Invest*. 2012;122(10):3416-3423.
11. Vegliante MC, Palomero J, Pérez-Galán P, et al. SOX11 regulates PAX5 expression and blocks terminal B-cell differentiation in aggressive mantle cell lymphoma. *Blood*. 2013;121(12):2175-2185.
12. Palomero J, Vegliante MC, Rodríguez ML, et al. SOX11 promotes tumor angiogenesis through transcriptional regulation of PDGFA in mantle cell lymphoma. *Blood*. 2014;124(14):2235-2247.
13. Zhang L, Yang J, Qian J, et al. Role of the microenvironment in mantle cell lymphoma: IL-6 is an important survival factor for the tumor cells. *Blood*. 2012;120(18):3783-3792.
14. Kurtova AV, Tamayo AT, Ford RJ, Burger JA. Mantle cell lymphoma cells express high levels of CXCR4, CXCR5, and VLA-4 (CD49d): importance for interactions with the stromal microenvironment and specific targeting. *Blood*. 2009;113(19):4604-4613.
15. Zhang H, Chen Z, Neelapu SS, Romaguera J, McCarty N. Hedgehog inhibitors selectively target cell migration and adhesion of mantle cell lymphoma in bone marrow microenvironment. *Oncotarget*. 2016;7(12):14350-14365.
16. Burger JA, Ford RJ. The microenvironment in mantle cell lymphoma: cellular and molecular pathways and emerging targeted therapies. *Semin Cancer Biol*. 2011;21(5):308-312.
17. Rajguru S, Kahl BS. Emerging therapy for the treatment of mantle cell lymphoma. *J Natl Compr Canc Netw*. 2014;12(9):1311-1318, quiz 1318.
18. Saba N, Wiestner A. Do mantle cell lymphomas have an 'Achilles heel'? *Curr Opin Hematol*. 2014;21(4):350-357.
19. Kim YR, Eom KS. Simultaneous inhibition of CXCR4 and VLA-4 exhibits combinatorial effect in overcoming stroma-mediated chemotherapy resistance in mantle cell lymphoma cells. *Immune Netw*. 2014;14(6):296-306.
20. Kahl BS, Spurgeon SE, Furman RR, et al. A phase 1 study of the PI3Kδ inhibitor idelalisib in patients with relapsed/refractory mantle cell lymphoma (MCL). *Blood*. 2014;123(22):3398-3405.
21. Rosich L, Montraveta A, Xargay-Torrent S, et al. Dual PI3K/mTOR inhibition is required to effectively impair microenvironment survival signals in mantle cell lymphoma. *Oncotarget*. 2014;5(16):6788-6800.
22. Zuber J, Rappaport AR, Luo W, et al. An integrated approach to dissecting oncogene addiction implicates a Myb-coordinated self-renewal program as essential for leukemia maintenance [published correction appears in *Genes Dev*. 2011;25(18):1997. *Genes Dev*. 2011;25(15):1628-1640.
23. Kawano Y, Kobune M, Yamaguchi M, et al. Ex vivo expansion of human umbilical cord hematopoietic progenitor cells using a coculture system with human telomerase catalytic subunit (hTERT)-transfected human stromal cells. *Blood*. 2003;101(2):532-540.
24. Enjuanes A, Albero R, Clot G, et al. Genome-wide methylation analyses identify a subset of mantle cell lymphoma with a high number of methylated CpGs and aggressive clinicopathological features. *Int J Cancer*. 2013;133(12):2852-2863.
25. Slack-Davis JK, Martin KH, Tilghman RW, et al. Cellular characterization of a novel focal adhesion kinase inhibitor. *J Biol Chem*. 2007;282(20):14845-14852.
26. Sulzmaier FJ, Jean C, Schlaepfer DD. FAK in cancer: mechanistic findings and clinical applications. *Nat Rev Cancer*. 2014;14(9):598-610.
27. Burger JA, Peled A. CXCR4 antagonists: targeting the microenvironment in leukemia and other cancers. *Leukemia*. 2009;23(1):43-52.
28. Herman SE, Lapalombella R, Gordon AL, et al. The role of phosphatidylinositol 3-kinase-δ in the immunomodulatory effects of lenalidomide in chronic lymphocytic leukemia. *Blood*. 2011;117(16):4323-4327.
29. Pérez-Galán P, Roué G, Villamor N, Montserrat E, Campo E, Colomer D. The proteasome inhibitor bortezomib induces apoptosis in mantle-cell lymphoma through generation of ROS and Noxa activation independent of p53 status. *Blood*. 2006;107(1):257-264.
30. Keasey MP, Kang SS, Lovins C, Hagg T. Inhibition of a novel specific neuroglial integrin signaling pathway increases STAT3-mediated CNTF expression. *Cell Commun Signal*. 2013;11:35.
31. Moreno MJ, Bosch R, Dieguez-Gonzalez R, et al. CXCR4 expression enhances diffuse large B cell lymphoma dissemination and decreases patient survival. *J Pathol*. 2015;235(3):445-455.
32. Olson TS, Ley K. Chemokines and chemokine receptors in leukocyte trafficking. *Am J Physiol Regul Integr Comp Physiol*. 2002;283(1):R7-R28.
33. Schaller MD. Cellular functions of FAK kinases: insight into molecular mechanisms and novel functions. *J Cell Sci*. 2010;123(7):1007-1013.
34. Burger JA, Bürkle A. The CXCR4 chemokine receptor in acute and chronic leukaemia: a marrow homing receptor and potential therapeutic target. *Br J Haematol*. 2007;137(4):288-296.
35. Burger JA, Burger M, Kipps TJ. Chronic lymphocytic leukemia B cells express functional CXCR4 chemokine receptors that mediate spontaneous migration beneath bone marrow stromal cells. *Blood*. 1999;94(11):3658-3667.
36. Le Y, Honczarenko M, Glodek AM, Ho DK, Silberstein LE. CXC chemokine ligand 12-induced focal adhesion kinase activation and segregation into membrane domains is modulated by regulator of G protein signaling 1 in pro-B cells. *J Immunol*. 2005;174(5):2582-2590.
37. Huang D, Khoe M, Befekadu M, et al. Focal adhesion kinase mediates cell survival via NF-kappaB and ERK signaling pathways. *Am J Physiol Cell Physiol*. 2007;292(4):C1339-C1352.
38. Bouchard V, Demers MJ, Thibodeau S, et al. Fak/Src signaling in human intestinal epithelial cell survival and anoikis: differentiation state-specific uncoupling with the PI3-K/Akt-1 and MEK/Erk pathways. *J Cell Physiol*. 2007;212(3):717-728.
39. Zhao J, Pestell R, Guan JL. Transcriptional activation of cyclin D1 promoter by FAK contributes to cell cycle progression. *Mol Biol Cell*. 2001;12(12):4066-4077.
40. Xu W, Li JY. SOX11 expression in mantle cell lymphoma. *Leuk Lymphoma*. 2010;51(11):1962-1967.
41. Jares P, Campo E. Advances in the understanding of mantle cell lymphoma. *Br J Haematol*. 2008;142(2):149-165.
42. Inamdar AA, Goy A, Ayoub NM, et al. Mantle cell lymphoma in the era of precision medicine-diagnosis, biomarkers and therapeutic agents. *Oncotarget*. 2016;7(30):48692-48731.
43. Xu L, Huang S, Hou Y, et al. Sox11-modified mesenchymal stem cells (MSCs) accelerate bone fracture healing: Sox11 regulates differentiation and migration of MSCs. *FASEB J*. 2015;29(4):1143-1152.

Downloaded from http://ashpublications.org/blood/article-pdf/130/4/501/1404829/blood776740.pdf by guest on 23 April 2024

44. Mitra SK, Hanson DA, Schlaepfer DD. Focal adhesion kinase: in command and control of cell motility. *Nat Rev Mol Cell Biol*. 2005;6(1):56-68.

45. Segarra M, Vilardell C, Matsumoto K, et al. Dual function of focal adhesion kinase in regulating integrin-induced MMP-2 and MMP-9 release by human T lymphoid cells. *FASEB J*. 2005;19(13): 1875-1877.

46. Ozkal S, Paterson JC, Tedoldi S, et al. Focal adhesion kinase (FAK) expression in normal and neoplastic lymphoid tissues. *Pathol Res Pract*. 2009;205(11):781-788.

47. Duxbury MS, Ito H, Zinner MJ, Ashley SW, Whang EE. Focal adhesion kinase gene silencing promotes anoikis and suppresses metastasis of human pancreatic adenocarcinoma cells. *Surgery*. 2004;135(5): 555-562.

48. Kane RC, Dagher R, Farrell A, et al. Bortezomib for the treatment of mantle cell lymphoma. *Clin Cancer Res*. 2007;13(18): 5291-5294.

49. Robak T, Huang H, Jin J, et al; LYM-3002 Investigators. Bortezomib-based therapy for newly diagnosed mantle-cell lymphoma. *N Engl J Med*. 2015;372(10):944-953.

50. Dal Col J, Zancai P, Terrin L, et al. Distinct functional significance of Akt and mTOR constitutive activation in mantle cell lymphoma. *Blood*. 2008;111(10):5142-5151.

51. Psyrri A, Papageorgiou S, Liakata E, et al. Phosphatidylinositol 3′-kinase catalytic subunit alpha gene amplification contributes to the pathogenesis of mantle cell lymphoma. *Clin Cancer Res*. 2009;15(18): 5724-5732.

Downloaded from http://ashpublications.org/blood/article-pdf/130/4/501/1404829/blood776740.pdf by guest on 23 April 2024